

# The anatomy of the bicipital tuberosity and distal biceps tendon

Augustus D. Mazzocca, MD,<sup>a</sup> Mark Cohen, MD,<sup>b</sup> Eric Berkson, MD,<sup>b</sup> Gregory Nicholson, MD,<sup>b</sup> Bradley C. Carofino, MD,<sup>a</sup> Robert Arciero, MD,<sup>a</sup> and Anthony A. Romeo, MD<sup>b</sup> Farmington, CT, and Chicago, IL

*The anatomy of the distal biceps tendon and bicipital tuberosity (BT) is important in the pathophysiology of tendon rupture, as well as surgical repair. Understanding the dimensions of the BT and its angular relationship to the radial head and radial styloid will facilitate surgical procedures such as reconstruction of the distal biceps tendon, radial head prosthesis implantation, and reconstruction of proximal radius trauma. We examined 178 dried cadaveric radii, and the following measurements were collected: radial length, length and width of the BT, diameter of the radius just distal to the BT, distance from the radial head to the BT, radial head diameter, width of the radius at the BT, radial neck-shaft angle, and styloid angle. Furthermore, the morphology of the BT ridge was defined as smooth (absent), small, medium, large, or bifid. Of the specimens, 48 were further analyzed with a computed tomography scanner at the level of the BT to determine the distance to traverse both the anterior and posterior cortex and the anterior cortex alone. Eighteen fresh-frozen cadaveric elbows were dissected, and the insertion footprint of the distal biceps tendon was defined. The BT has a mean length of  $22 \pm 3$  mm and a mean width of  $15 \pm 2$  mm. The tendon insertion footprint is a ribbon-shaped configuration on the most ulnar aspect of the BT, and it occupies 63% of the length and 13% of the width of the BT. The BT ridge is absent in 6% of specimens and bifid in 6%, and the remaining 88% of specimens have a single ridge that may be classified as small, medium, or large. The mean diameter of the radial head is  $22 \pm 3$  mm. The mean radial neck-shaft angle is  $7^\circ \pm 3^\circ$ ,*

*and the mean BT-radial styloid angle is  $123^\circ \pm 10^\circ$ . None of the measurements correlated with patient age, sex, or race. We concluded that the morphology of the BT ridge is variable. The insertion footprint of the distal biceps tendon is on the ulnar aspect of the BT ridge. The dimensions of the radius and BT are applicable to several surgical procedures about the elbow. (J Shoulder Elbow Surg 2007;16:122-127.)*

**T**he recognition and treatment of distal biceps tendon ruptures have increased over time. Previously, this injury was considered rare; only 65 cases were reported before 1941.<sup>2,4</sup> However, a more recent retrospective study identified the incidence to be 1.2 per 100,000.<sup>10</sup> The literature on this topic has similarly expanded. A MEDLINE search identified 53 articles on the distal biceps tendon published since 1995, whereas only 58 had been produced in the previous 25 years.<sup>8</sup>

Mechanical failure of the distal biceps tendon at its insertion may be multifactorial in origin. However, the structural anatomy of the tendon at the bicipital tuberosity has been implicated. It has been suggested that a prominent edge of the tuberosity erodes the tendon during pronation, rendering it vulnerable to rupture when exposed to high forces.<sup>1,11</sup> This may be analogous to acromial morphology and rotator cuff tears. Previously, the anatomy of the biceps tendon insertion on the radius has received little attention. Koch and Tillmann<sup>6</sup> reported that the biceps inserts over an area of 3 cm<sup>2</sup>. However, more detailed data on the insertion footprint and its relationship to tuberosity morphology have never been reported.

The purpose of this study is to define the external and internal osteology of the bicipital tuberosity as it relates to the biceps tendon insertion. Hopefully, this information will aid in our understanding and surgical treatment of distal tendon ruptures and other conditions about the proximal radius.

## MATERIALS AND METHODS

A total of 178 dried cadaveric radii (89 pairs) from both male and female specimens were examined from the

From the <sup>a</sup>Department of Orthopaedic Surgery, University of Connecticut, Farmington, and <sup>b</sup>Department of Orthopaedic Surgery, Rush University Medical Center, Chicago.

Financial support provided by Arthrex (Naples, FL).

Reprint requests: Bradley C. Carofino, MD, 28 Walbridge Rd, West Hartford, CT 06119 (E-mail: bradcarofino@yahoo.com)

Copyright © 2007 by Journal of Shoulder and Elbow Surgery Board of Trustees.

1058-2746/2007/\$32.00

doi:10.1016/j.jse.2006.04.012

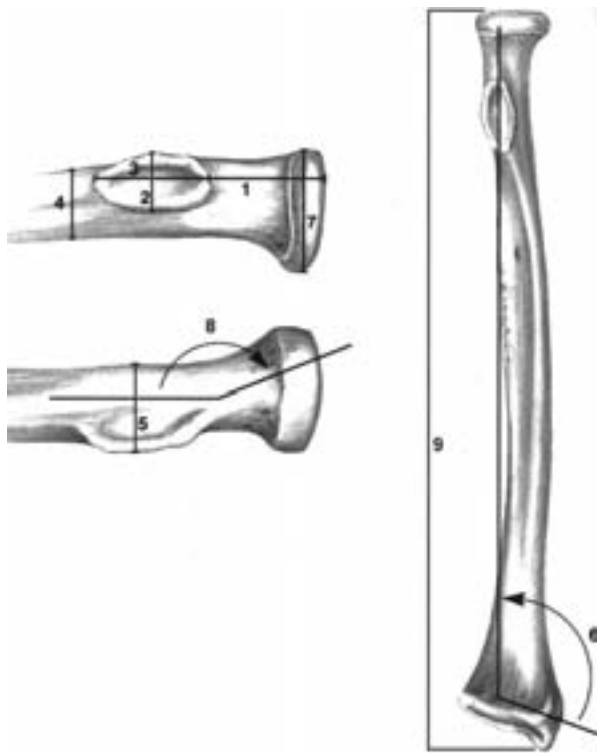


**Figure 1** The external osteology of the radius and tuberosity was defined by 9 measurements: the distance from the proximal portion of the radial head to the beginning of the bicapital tuberosity (1), width of the tuberosity (2), length of the tuberosity (3), diameter of the radius just distal to the tuberosity (4), width of the radius at the level of the bicapital tuberosity (5), styloid angle (6), radial head diameter (7), radial neck-shaft angle (8), and radial length (9).

Hamann-Todd Human Osteological Collection at the Cleveland Museum of Natural History, Cleveland, OH. Of the specimens, 70% came from individuals aged between 40 and 59 years, 20% came from individuals aged between 20 and 39 years, and 10% came from individuals aged between 60 and 69 years. Seventy-five percent of the specimens were from men, and twenty-five percent were from women. Eighteen additional fresh cadaveric specimens were used to obtain data on the biceps tendon insertion relative to bony landmarks. Of these, 12 were from men and 6 were from women, with a mean age of  $67 \pm 5$  years.

#### External osteology

The dimensions of the radius and the tuberosity were defined by the following measurements: the distance from the proximal portion of the radial head to the beginning of the bicapital tuberosity, the width of the tuberosity, the length of the tuberosity, the diameter of the radius just distal to the tuberosity, the width of the radius at the level of the bicapital tuberosity, the radial head diameter, and the length of the radius. All measurements are defined in Figure 1.

Angular measurements included the radial neck-shaft angle and the styloid angle (Figure 1, dimensions 6 and 8). The styloid angle is formed by a line that is parallel to the

long axis of the tuberosity and a second line that bisects the radial styloid. This angle defines the torsional relationship of the bicapital tuberosity to the radial styloid at the wrist.

Radial length was measured by use of an osteometric measuring device provided by the Cleveland Museum of Natural History. All other measurements were made with a digital caliper (C. E. Johansson, Eskilstuna, Sweden). Angular measurements were made with a goniometer. The intraobserver and interobserver reliability of these measurements was determined in a pilot experiment using 4 specimens and found to be suitable for the purposes of the experiment. The reproducibility of measurements was consistently limited by interobserver reliability. Measurements of distance were reproducible within  $\pm 0.8$  mm and angular measurements within  $\pm 5^\circ$ . The intraobserver reliability was  $\pm 0.3$  mm for distance measurements and  $\pm 2^\circ$  for angular measurements.

Finally, the morphology of the bicapital tuberosity was characterized with respect to a variable ridge identified on its ulnar aspect. This ridge was classified as smooth (no ridge), a single ridge, or a bifid ridge (Figure 2). These 3 categories were grossly distinct. The radii with a single-ridge tuberosity were further classified as having a small, medium, or large ridge, which was a qualitative assessment.

#### Computed tomography measurements

Of the 178 specimens, 48 underwent further analysis with a computed tomography (CT) scanner (Somatom Volume Zoom model; Siemens, Erlangen, Germany). The proximal radii were imaged with 0.5-mm slices, with image reconstructions every 1 mm. The distal radii were scanned with 3-mm slices. The internal osteology of the bicapital tuberosity was measured in the coronal and sagittal planes. Specifically, the distances required to traverse the radius by passing through both cortices (bicortical distance) and through only 1 cortex (unicortical distance) were quantified. Scans taken at the level of the midpoint of the tuberosity were used for these measurements (Figure 3). Finally, the styloid angle was measured from axial sections by drawing a line through the midpoint of the bicapital tuberosity and another through the midpoint of the radial styloid and measuring the resultant angle (Figure 1, dimension 6).

#### Cadaveric dissections

Eighteen fresh-frozen cadavers were dissected under loupe magnification. The anatomy of the distal biceps tendon insertion at the bicapital tuberosity was recorded and the length and width of the footprint quantified by use of digital calipers.

#### Statistics

All data were entered into the SPSS statistical software package (version 10; SPSS, Chicago, IL). The Levene test for equality of variances was used to evaluate correlations between osteology and patient demographics (age, race, and sex).

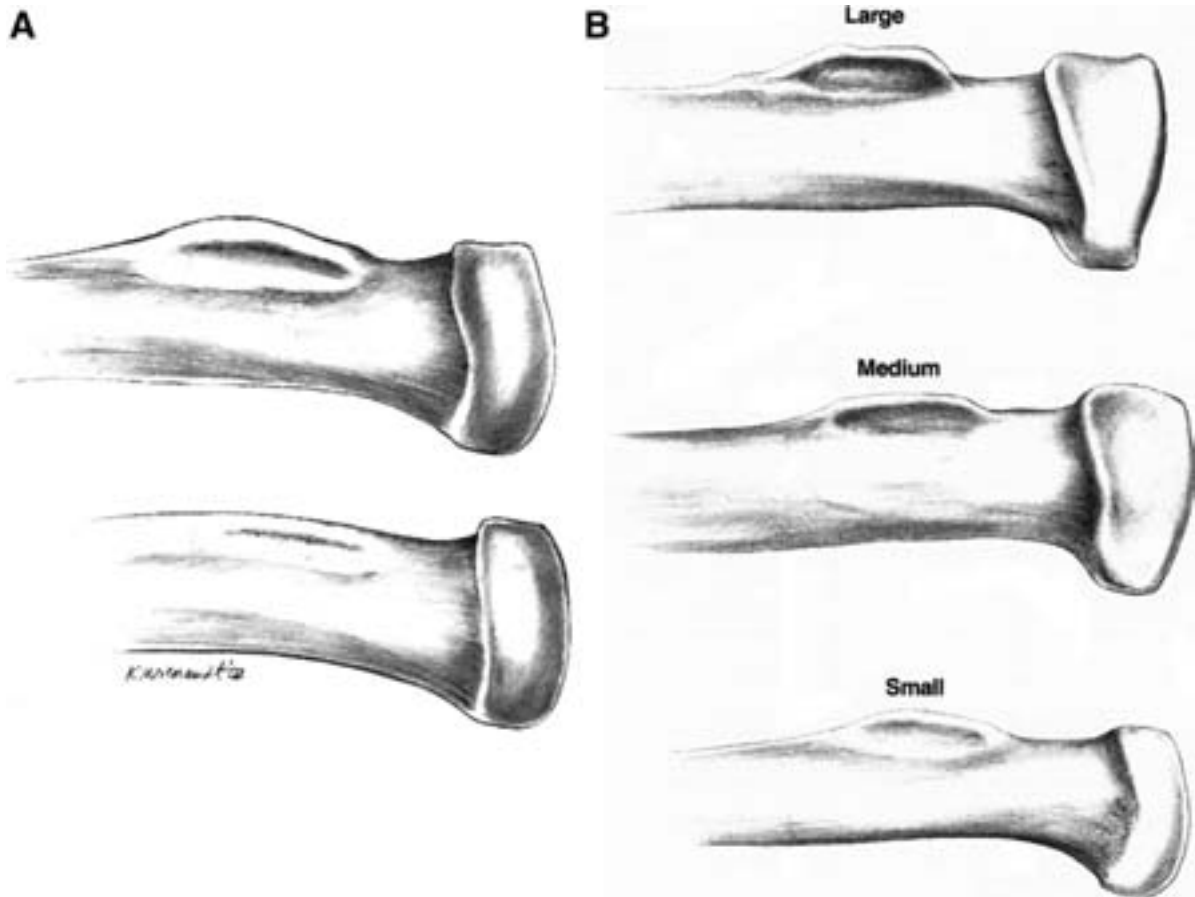


**Figure 2** **A**, The bifid ridge type (*top*) has two prominent ridges, one medial and lateral, with a trough in between. *Bottom*, Smooth (no ridge) type. **B**, The single-ridge type was separated into 3 subtypes based on qualitative appearance: small, medium, and large.



**Figure 3** The unicortical (1) and bicortical (2) distances were measured from a coronal CT image taken through the midpoint of the tuberosity. The same measurements were also taken from sagittal images (not shown).

## RESULTS

### External osteology

The dimensions of the bicipital tuberosity and radius, as directly measured from specimens, are presented in [Table 1](#). On average, the bicipital tuberosity has a length of  $22 \pm 3$  mm and a width of  $15 \pm 2$  mm ([Figure 1](#), dimensions 2 and 3). The diameter of the radial head is  $23 \pm 2$  mm ([Figure 1](#), dimension 7). The radial neck-shaft angle is  $7^\circ \pm 3^\circ$ , and the styloid angle is  $123^\circ \pm 10^\circ$  ([Figure 1](#), dimensions 6 and 8). The remaining measurements are presented in [Table 1](#). There was no correlation between any of the 9 anatomic measurements and the age, race, or gender of the subject ( $P < .05$ ).

The prevalence of each tuberosity ridge type was as follows: A single ridge (either small, medium, or large) was present in 88% of specimens, a smooth type (no ridge) was present in 6%, and a bifid ridge was present in 6%. Of the specimens in the single-ridge tuberosity group, 12% had a large ridge, 41% had a small ridge, and 47% had a medium ridge.

**Table I** External osteology measurements

Measurement	Mean ± SD	Minimum	Maximum
Distance from radial head to BT (mm)	25 ± 3	19	30
BT width (mm)	15 ± 2	10	19
BT length (mm)	22 ± 3	16	30
Diameter of radius distal to BT (mm)	17 ± 2	13	22
Width of radius at BT (mm)	17 ± 2	12	23
Styloid angle (°)	123 ± 10	98	142
Radial head diameter (mm)	23 ± 2	18	28
Radial neck-shaft angle (°)	7 ± 3	0	14
Radial length (mm)	24 ± 2	20	27

BT, Bicipital tuberosity.



**Figure 4** Large ridge type.

There was no correlation between tuberosity type and age decade, gender, or race. The various ridge types are presented in Figures 4 through 8.

#### CT osteology

When the radii were imaged in the coronal plane, the bicortical thickness averaged  $15 \pm 1$  mm. The unicortical thickness—that is, the distance to traverse the anterior cortex but not the posterior cortex—was  $13 \pm 1$  mm. These measurements are defined in Figure 3. The styloid angle was  $124^\circ \pm 11^\circ$ . The internal osteology measurements were also taken from sagittal CT images, and the results are presented in Table II.

#### Cadaveric dissection and soft-tissue tuberosity footprint

The distal biceps tendon inserted on the ulnar side of the tuberosity. The insertion footprint is a ribbon-



**Figure 5** Medium ridge type.



**Figure 6** Small ridge type.



**Figure 7** Smooth ridge type.

shaped strip with a mean length of  $14 \pm 2$  mm and a mean width of  $2 \pm 0.3$  mm (Figure 9). On the basis of the dimensions of the tuberosity, the tendon inser-



**Figure 8** Bifid ridge type.

**Table II** Internal osteology measurements taken by CT

Measurement	Mean $\pm$ SD	Minimum	Maximum
Unicortical distance:			
Coronal (mm)	13 $\pm$ 1	9	16
Bicortical distance:			
Coronal (mm)	15 $\pm$ 1	12	18
Styloid angle:			
Coronal (mm)	124 $\pm$ 11	153	95
Unicortical distance:			
Sagittal (mm)	14 $\pm$ 2	9	18
Bicortical distance:			
Sagittal (mm)	16 $\pm$ 2	11	20

tion occupies approximately 63% of the length of the tuberosity and 13% of the width. The remainder of the tuberosity is roughened and covered by an overlying bursa present on the radial side of the tendon. The insertion footprint does not cover the ridge.

## DISCUSSION

The anatomy of the distal biceps tendon and bicipital tuberosity is relevant to tendon rupture and repair. Microscopically, the biceps tendon is composed of 2 portions. There is a traction-type portion on the ulnar aspect of the tendon and a gliding portion on the radial side, which abuts the bursa.<sup>5,6</sup> It has been suggested that chronic inflammation of the bursa may predispose a patient to tendon rupture. It has also been hypothesized that the bicipital tuberosity may contribute to tendon rupture. Davis and Yassine<sup>1</sup> reported that there is a knife-like margin of the tuberosity causing erosion of the tendon during forearm rotation. This concept is supported by the fact that the space available for the tendon between the ulna and radius decreases by approximately 50% during pro-

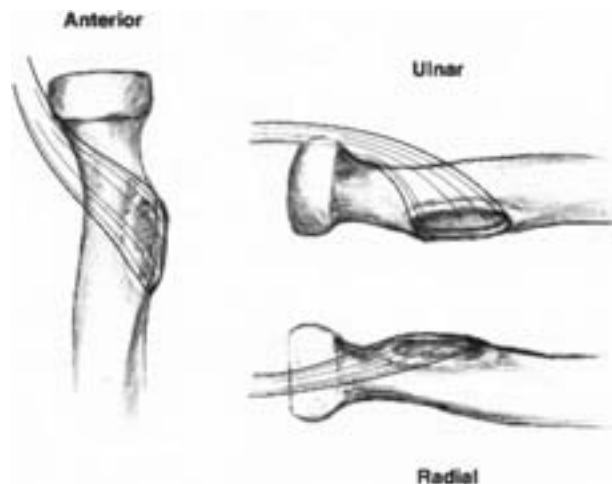


**Figure 9** The distal biceps tendon inserts on the ulnar aspect of the tuberosity as a ribbon-shaped insertion footprint.

duction, and irregularity of the tuberosity has been reported in patients in whom rupture occurs.<sup>1,9,11</sup>

To our knowledge, this study is the first to categorize the morphologic variants of the bicipital tuberosity and tendon insertion. We found that the majority of individuals have a single ridge, which is either of the small or medium type. The smooth (no ridge) morphology was not uncommon, yet we have never encountered this morphology in a patient with a distal biceps tendon rupture. Furthermore, we are not aware of any such reports in the literature. A large ridge was seen in 11% of specimens, independent of age or gender.

This is the first report to define clearly the anatomy of the biceps tendon insertion with respect to the radial tuberosity. We found that the biceps tendon passes over the ridge of the tuberosity to insert on its ulnar aspect; the footprint does not include the ridge. The distance spanned by the tendon over the raised ridge likely functions as a pulley, increasing the mechanical advantage of the musculotendinous unit. Current techniques of distal biceps tendon repair that involve shortening of the tendon for placement into a bony trough may theoretically diminish this advantage of the tuberosity. However, it should be noted that present studies have not demonstrated a reduction in flexion or supination strength associated with shortening of the muscle-tendon unit to place it inside a bony trough.<sup>3</sup> Nonetheless, we believe that it is beneficial to maximize the mechanical advantage of the repair, and therefore, we advocate an anatomic repair of the tendon to its original configuration.

We have catalogued the mean measurements for relevant dimensions of the proximal radius and bicipital tuberosity, as well as the angular relationship between structures. These have implications for future

techniques of biceps tendon repair, as well as forearm bone trauma and reconstruction.<sup>7</sup>

We thank Dr Bruce Latimer and Lyman Jellema, who are associated with the Hamann-Todd Human Osteological Collection at the Cleveland Museum of Natural History, for their tremendous help and cooperation in collecting the data for this report. We also thank Tae-Ho Lim, PhD, for the use of the Biomechanics Laboratory at Rush University, as well as Dr Betina Fabrice and Eric Lorenze for their technical and editorial assistance.

#### REFERENCES

1. Davis WM, Yassine Z. An etiological factor in tear of the distal tendon of the biceps brachii. Report of two cases. *J Bone Joint Surg Am* 1956;38:1365-8.
2. Dobbie RP. Avulsion of the lower biceps brachii tendon. Analysis of 51 previously unreported cases. *Am J Surg* 1941;51:662-3.
3. El-Hawary R, Macdermid JC, Faber KJ, Patterson SD, King GJ. Distal biceps tendon repair: comparison of surgical techniques. *J Hand Surg [Am]* 2003;28:496-502.
4. Johnson S. Avulsion of biceps tendon from the radius. *N Y Med J* 1897;66:261-2.
5. Kannus P, Jozsa L. Histopathological changes preceding spontaneous rupture of a tendon. A controlled study of 891 patients. *J Bone Joint Surg Am* 1991;73:1507-25.
6. Koch S, Tillmann B. The distal tendon of the biceps brachii. Structure and clinical correlations. *Ann Anat* 1995;177:467-74.
7. Mazzocca AD, Bicos J, Arciero RA, Romeo AA, Cohen MS, Nicholson G. Repair of distal biceps tendon rupture using a combined anatomic interference screw and cortical button. *Tech Shoulder Elbow Surg* 2005;6:108-15.
8. MEDLINE [online database]. Bethesda (MD): US National Library of Medicine; 2006.
9. Morrey BF. The elbow and its disorders. 3rd ed. Philadelphia: Saunders; 2000.
10. Safran MR, Graham SM. Distal biceps tendon ruptures incidence, demographics and the effect of smoking. *Clin Orthop Relat Res* 2002;404:275-83.
11. Seiler JG III, Parker LM, Chamberland PD, Sherbourne GM, Carpenter WA. The distal biceps tendon. Two potential mechanisms involved in its rupture: arterial supply and mechanical impingement. *J Shoulder Elbow Surg* 1995;4:149-56.

## ERRATUM

---

The journal wishes to point out that there was an inadvertent duplicate publication of same article with slightly different titles.<sup>1,2</sup> There was no intent in any way on the part of the authors to publish the article in duplicate, and the journal regrets the error. The second of the two articles has been withdrawn from the electronic publication site.

1. Sanchez-Sotelo J, O'Driscoll SW, Morrey BF. Medial oblique compression fracture of the coronoid process of the ulna. *J Shoulder Elbow Surg* 2005;14:60-64.
2. Sanchez-Sotelo J, O'Driscoll SW, Morrey BF. Anteromedial Compression Fracture of the Coronoid Process of the Ulna. *J Shoulder and Elbow Surg* 2006;15:e5-e8.